High-Pressure Liquid Injection for Reciprocating Compressors to Improve Efficiency and Operating Range

Jonas SCHMITT[1*], Robin LANGEBACH[1]

[1] Karlsruhe University of Applied Sciences,
The Schaufler Foundation Professorship for Compressor Technology,
Institute for Refrigeration, Air Conditioning and Environmental Technology
76133 Karlsruhe, Germany
Phone: +49 721 925 2128 Email: jonas.schmitt@h-ka.de

ABSTRACT

Isentropic or above-isentropic compression in a vapor compression cycle can result in compressor discharge temperatures exceeding the condensing temperature, depending on the refrigerant's thermophysical properties, initial state and operating conditions. This discharge superheat is unfavorable in terms of both second law efficiency and practical application limits. Heat rejection during the compression can shift the process towards the ideal Carnot cycle, thereby improving cycle efficiency and operating limits due to reduced outlet temperatures. However, due to a comparably high compression frequency and small heat transfer area, the heat rejection through the working chamber walls is often insufficient to achieve substantial temperature reduction. For compressors that can tolerate significant amounts of liquid in their working chamber, particularly screw and scroll compressors, effective temperature reduction can be achieved by direct oil or refrigerant injection. For reciprocating compressors, similar approaches are only applicable to a very limited extent due to the risk of liquid slugging.

This study presents a method for high-pressure liquid refrigerant injection for reciprocating compressors, which employs a high-pressure pump and a controllable injection valve in the working chamber. The atomization of the injected refrigerant allows for a rapid evaporation, preventing liquid slugging and achieving significant temperature reduction in the working chamber. By controlling the injection rate through variable injection valve timing, the temperature profile during compression can be adjusted.

The coupled compression-injection is assessed using an energetic chamber model, and the influence of injection quantity and injection rate on efficiency and discharge temperature is assessed. Technical implications regarding compressor operating limits and injection pressure are outlined.

In summary, this study introduces a novel approach for enhancing reciprocating compressor efficiency by employing high-pressure liquid refrigerant injection. The theoretical evaluation of this coupled compression-injection system highlights its potential to achieve significant discharge superheat reduction and – in particular cases – improve the efficiency.

1. INTRODUCTION

The entropy production in reciprocating refrigeration compressor usually exceeds the entropy rejection with heat transfer to the environment. As a result, the indicated work and the outlet temperature is higher for a real compression process compared to adiabatic, isentropic compression. However, even isentropic compression is not thermodynamically ideal, depending on the refrigerant. For refrigerants with a shallow dew line slope, e.g. R-717 (ammonia), the compressor discharge temperature with isentropic compression significantly exceeds the condensing temperature. The difference between discharge and condensing temperature can be referred to as discharge superheat. During the de-superheating of the hot gas from discharge to condensing temperature, exergy is lost to the heat sink, reducing the cycle efficiency. Furthermore, high discharge superheat reduces the operating range of a compressor, because excessive discharge temperature can result in a degradation of the compressor oil, among other problems.

Extensive research has been conducted on compressor cooling in recent years (Kim *et al.*, 2022). Effective methods for temperature reduction include vapor and liquid injection for scroll compressors, either at the suction port (Lee *et al.*, 2015) or directly into the working chamber (Cho *et al.*, 2003; Dutta *et al.*, 2001), as well as oil injection for

both screw (Abdan *et al.*, 2019; Basha *et al.*, 2021) and scroll compressors (Bell *et al.*, 2011, 2013). Oil injection was also investigated for reciprocating compressors, and reduced discharge temperature, but also reduced efficiency was found (Kremer *et al.*, 2008, 2012). Recently, a new approach of vapor injection into the working chamber of reciprocating compressors in refrigeration systems with multiple evaporation pressure levels was proposed, which promises a significant efficiency improvement (Liang *et al.*, 2023).

It can be seen that reciprocating compressors lack effective methods for temperature reduction compared to other compressors types. Therefore, a process for high-pressure liquid injection for reciprocating compressors is proposed. In this process, liquid refrigerant from the condenser outlet is brought to a pressure level above the condensing pressure using a pump. The high pressure refrigerant is then injected into the working chamber through an injection valve, similar to injectors used in direct injection combustion engines. Compared to existing approaches, that utilize an existing pressure level in the system, two main advantages are expected for the high pressure injection:

1. The injection pressure level is always above the chamber pressure. In combination with the valve's adjustable injection timing, this allows an injection at any point of the compression cycle and a control of the injected mass.
2. Given a large enough pressure difference, the injected refrigerant is atomized when exiting the injection nozzle. This facilitates fast evaporation and cooling in the chamber, and prevents liquid slugging.

The basics of a similar process for refrigeration systems were first outlined by Holtzapple in 1989, based on a patent from 1946 (Rouleau, 1946; Holtzapple, 1989). Even though the study found a significant potential for efficiency improvement with certain refrigerants, especially R-717, the concept has, to the authors' knowledge, not been pursued since the original publication.

In the following sections, the concept of high-pressure refrigerant injection is described in detail, including its effect on energy efficiency and its impact on the refrigeration system's components.

2. HIGH PRESSURE INJECTION PROCESS

2.1 Process Setup

The cycle setup for the proposed refrigerant injection is shown in Figure 1. The injected process is based on a regular vapor compression cycle with compressor (1 → 2), condenser (2 → 3), expansion valve (3 → 4), and evaporator (4 → 1). As additional components, a liquid receiver at the condenser outlet, a refrigerant pump (3 → 5) and an injection valve for each cylinder located in the cylinder head are required. Saturated or slightly subcooled liquid enters the pump from the liquid receiver. The pump compresses the refrigerant to a pressure above the condensing pressure and feeds the high-pressure refrigerant to the injection valve. Through the injection valve, the refrigerant is injected into the compressor chamber, during which it is isenthalpically expanded to the current (transient) chamber pressure (5 → 6). Depending on the pump type and control strategy, additional components such as a pulsation damper and pressure relief valve may be required, which are shown in light gray.

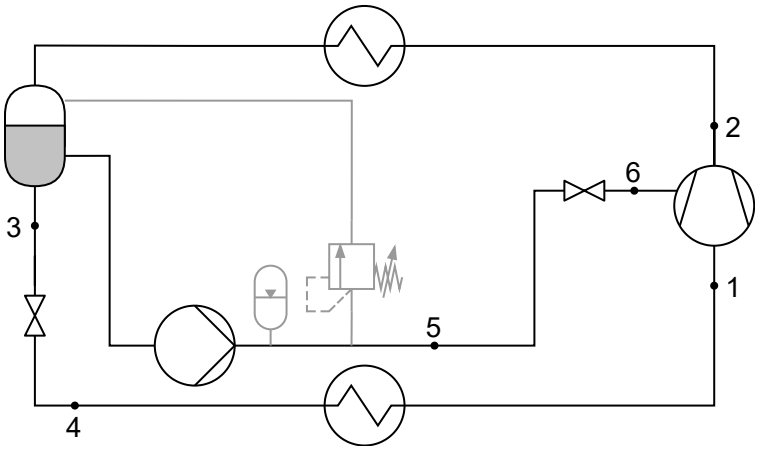

Figure 1: Cycle setup for high-pressure liquid injection

2.2 Thermodynamic Principle of the Coupled Injection-Compression Process

The model of a constant volume chamber will be used to explain the working principle of the liquid injection. It is assumed that a chamber with a constant volume V_{chamb} is filled with superheated vapor at a pressure p_{gas} and temperature T_{gas}. Into this chamber, refrigerant is injected through an injection nozzle. At the nozzle entry, this injected refrigerant is at a pressure level above the chamber pressure and in the state of subcooled liquid. Through the nozzle, the refrigerant is isenthalpically expanded to the chamber pressure, so that the refrigerant is a two-phase mixture of liquid and gas, with a vapor quality x_{inj}, at the nozzle outlet. Therefore, the temperature of the injected refrigerant is the saturation temperature T_{sat} for the current chamber pressure, while the T_{gas} is above the saturation temperature, $T_{gas} > T_{sat}$. After some time, the injected refrigerant has completely mixed and the chamber is again in a thermal equilibrium. Depending on the relative injected mass, the new state can either still be superheated or a two-phase mixture with $x_{mix} > x_{inj}$. In any case, the new equilibrium temperature T_{mix} is lower than the initial temperature T_{gas}.

However, the injection not only has an influence on the temperature in the chamber, but also on the pressure. It is known that for a gas enclosed in a constant volume, the pressure is proportional to temperature and mass:

$$p \propto m \cdot T \tag{1}$$

On one hand, the mass in the chamber increases, which would result in a pressure increase for an isothermal process. On the other hand, as shown above, the temperature decreases with the injection, where a temperature decrease results in a pressure reduction for a constant mass process. Therefore, the injection can result in an increase or decrease of chamber pressure, depending on whether the influence of mass or temperature predominates. To evaluate the pressure at equilibrium after injection, an energy balance can be used:

$$u_{mix} \cdot (m_{gas} + m_{inj}) - u_{gas} \cdot m_{gas} = h_{inj} \cdot m_{inj} \tag{2}$$

(2) can be solved for the specific energy u_{mix}:

$$u_{mix} = \frac{h_{inj} \cdot m_{inj} + u_{gas} \cdot m_{gas}}{m_{gas} + m_{inj}} \tag{3}$$

Additionally, the density

$$\varrho_{mix} = \frac{m_{gas} + m_{inj}}{V_{chamb}} \tag{4}$$

can be calculated. From density and specific energy, all other thermal properties of the new thermal equilibrium state can be calculated using a fluid properties database such as CoolProp or REFPROP. The pressure difference $p_{mix} - p_{gas}$ is a function of operating conditions, relative injected mass, and fluid properties. It is found that the injection usually results in a reduced pressure for refrigerants with large evaporation heat. This is because for those refrigerants only a relatively small amount of refrigerant needs to be injected to achieve the cooling effect.

To move on from the constant chamber model to a process with compression, i.e. decreasing volume, it can simply be assumed that the chamber volume is reduced by an infinitesimal amount after the mixture has reached a steady state. This change in volume requires some work to be carried out on the volume by the piston, i.e. the compression work. After the compression, another step with injection and mixing follows, and after that another compression step. By linking multiple compression and injection steps in that manner, a quasi-continuous process with simultaneous injection and compression is approximated.

2.3 Effect on Compressor and Cycle Efficiency

The effect of liquid injection on the compression process is calculated using an angle-discrete energetic chamber model based on the considerations from section 2.2. A detailed description of the model was published by Schmitt and Langebach (2024). The model presupposes an idealized compression process, i.e. isentropic and adiabatic compression, no valve pressure loss and no suction superheat, as well as an idealized injection process, i.e. an instantaneous evaporation and mixing of the injected refrigerant. The model is therefore not an ideal representation of the actual process, as in reality the rate of evaporation and mixing is limited by heat and mass transfer in the working chamber. However, in the authors' opinion, the model is well suited to make a prediction regarding the theoretical potential of the injection. CoolProp version 6.6.0 is used as the fluid properties database.

The efficiency of a vapor compression refrigeration cycle is generally defined as the ratio of work input rate P, i.e. electrical work or shaft work, to the heat intake rate in the evaporator $\dot{Q}_\mathrm{o}$, given as the *COP*:

$$COP = \frac{\dot{Q}_\mathrm{o}}{P} \tag{5}$$

In case of the high-pressure injection process, the work input rate P comprises the compressor, pump, and injection valve. However, the drive power for pump and injection valve were found to be negligible relative to the compressor and will therefore be omitted hereafter. For the high-pressure injection, it is more appropriate to consider the energy quantities per revolution rather than comparing flow rates:

$$\varepsilon = \frac{m_\mathrm{suc} \cdot (h_1 - h_4)}{W} \tag{6}$$

The evaporation energy per revolution is thereby derived from the enthalpy difference between compressor inlet h_1 and expansion valve outlet h_4 and the mass intake through the suction valve per revolution m_suc. For an ideal compressor without suction valve losses and clearance volume, m_suc is only a function of the displacement and the suction gas density. It can therefore be assumed to be constant for a given refrigerant, evaporation pressure, and compressor geometry, again assuming no suction superheat, and it is sufficient to only evaluate the compression work W. The compression work per revolution is the indicated work, given as the closed integral over the pressure-volume curve. It can be visualized as the area enclosed by the compression process in the p, V-indicator plot. A smaller enclosed area equals less compression work and therefore increased cycle efficiency under the above made assumptions. With that, the effect of the liquid injection becomes apparent from the constant volume chamber model: depending on refrigerant and working point, the injection can result in a pressure reduction for a given chamber volume. This is expressed in the indicator plot in the form of a flatter pressure curve during compression, and therefore a reduced area and increased efficiency.

The effect on the indicator plot is shown for a theoretical example in Figure 2a. Here, a regular isentropic (adiabatic) compression is compared to a so-called ”dew line compression”, where just enough refrigerant is injected to cool the compressed gas to close to the saturated state. The resulting process is visualized in the T, s-plot in Figure 2b. Both processes start at the evaporation pressure p_o at the dew line and end at the condensing pressure p_c. But while the end point of the isentropic compression is superheated, the end point for dew line compression is at the dew line. It can clearly be seen in the p, V-plot, that the dew line compression process encloses a smaller area and thus requires less compression work per revolution.

2.4 Efficiency Increase for Various Operating Points, Refrigerants, and Injection Strategies

The specific compression work

$$w = \frac{W}{m_\mathrm{suc}} \tag{7}$$

for the coupled injection-compression process is calculated for various operating points, refrigerants, and injection strategies, and compared to the ideal compression process. For refrigerants with an anterograde dew line, the ideal compression process is the isentropic-isothermal compression, as proposed by Langebach *et al.* (2024). These refrigerants are characterized by a typical bell-shaped vapor dome, where the dew line entropy at the evaporating pressure s''_o is larger than at the condensing pressure s''_c. Examples are R717, R-744 (CO_2), and R-32. The specific isentropic-isothermal compression work $w_\mathrm{is,it}$ for these refrigerants can be calculated from the entropy and enthalpy at the dew line and the condensing temperature:

$$w_\mathrm{is,it} = h''_\mathrm{c} - h''_\mathrm{o} - T_\mathrm{c} \cdot (s''_\mathrm{c} - s''_\mathrm{o}) \tag{8}$$

Refrigerants with a retrograde dew line such as R-600a (isobutane) and other long chain hydrocarbons, where s''_c is larger than s''_o, do not benefit from the injection under the assumption of an idealized process and are therefore not evaluated further. Using the work for isentropic-isothermal compression, the isentropic-isothermal efficiency $\eta_\mathrm{is,it}$ can be calculated:

$$\eta_\mathrm{is,it} = \frac{w}{w_\mathrm{is,it}} \qquad \eta^\mathrm{is}_\mathrm{is,it} = \frac{w_\mathrm{is}}{w_\mathrm{is,it}} \tag{9}$$

To evaluate the effect of the injection, the change in $\eta_\mathrm{is,it}$ relative to the efficiency for the isentropic process $\eta^\mathrm{is}_\mathrm{is,it}$ is calculated.

$$\frac{\eta_\mathrm{is,it} - \eta^\mathrm{is}_\mathrm{is,it}}{\eta^\mathrm{is}_\mathrm{is,it}} \tag{10}$$

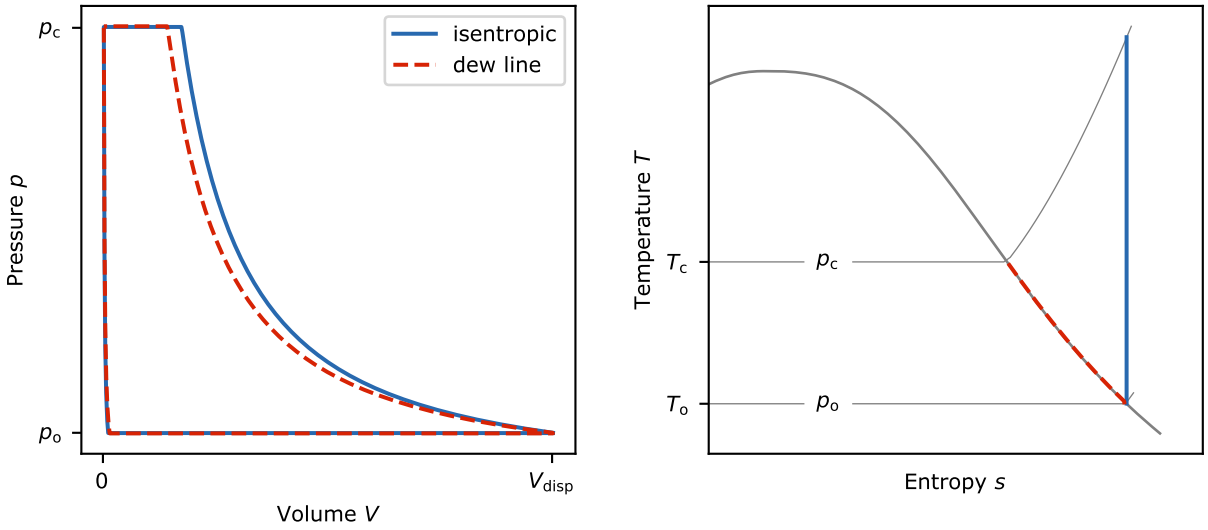

(a) Pressure-Volume p, V-plot

(b) Temperature-Entropy T, s-plot

Figure 2: Exemplary plots for isentropic compression and dew line compression with injection

Regarding the injection rate, five different theoretical profiles are evaluated:

1. **isentropic**: regular isentropic (adiabatic) compression without injection as baseline
2. **dew line**: injection rate adjusted to achieve a compression process along the dew line, see Figure 2
3. **constant**: constant injection rate, with injection during the full compression stroke and equal injected mass as ”dew line” process
4. **reduced**: same as ”constant” process, but with injection rate reduced to 20 %
5. **burst**: short injection burst with identical injection rate as ”constant” process, but only during 20 % of the compression stroke

The compression processes in a T, s-plot and the respective relative injection rates are shown in Figure 3. The relative injection rate is the current mass flow rate relative to the flow rate for the ”constant” process. Some conclusions can already be drawn from these figures. The total injected mass is equal for the ”dew line” and ”constant” process and for the ”reduced” and ”burst” process respectively. Consistent with this, the compressor outlet state is identical for these processes, while the T, s-curve is different. It can therefore be assumed that the compressor outlet state mainly depends on the total injected mass, rather than the injection profile.

t_o	t_c	**source**		**use case**	**designation**
-31.6 °C	40.5 °C	AHRI 540	(AHRI, 2020)	deep-freezing	DF
-10 °C	45 °C	DIN EN 12900	(DIN e.V., 2013)	normal-freezing	NF
7.2 °C	54.4 °C	AHRI 540	(AHRI, 2020)	heat pump low	HP L
40 °C	90 °C	-		heat pump high	HP H

Table 1: Selected operating points

In Figure 4a the improvement of $\eta_{is,it}$ for R-717 for the various injection profiles compared to isentropic compression is shown. The operating points are defined as shown in Table 1. Keeping in line with the previous observations, it can be seen that the total injected mass is again the main factor. The ”dew line” and ”constant” processes achieve a similar improvement, while the result for the ”burst” and ”reduced” processes is reduced but similar among those.

In Figure 4b, the efficiency improvement is shown for various refrigerants and operating points. It can be seen that from

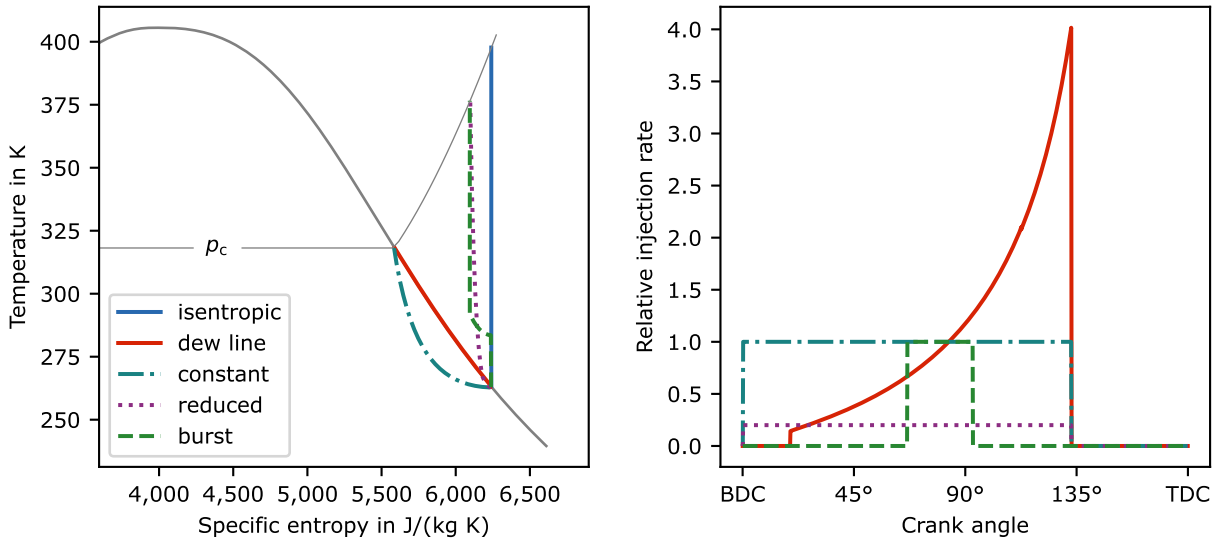

(a) Compression process in T, s-plot

(b) Relative injection rate

Figure 3: Various injection profiles with R-717

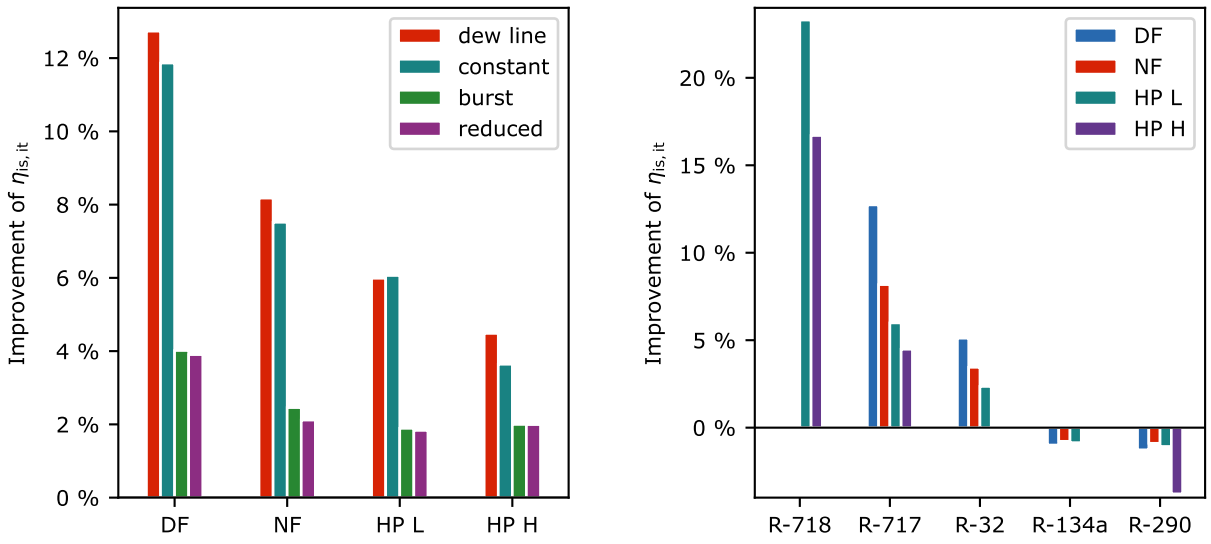

(a) Variation of injection strategy and operating point with R-717

(b) Variation of fluid and operating point with ”dew line” injection

Figure 4: Improvement of isentropic-isothermal efficiency trough high-pressure liquid injection

the examined refrigerants, R-718 (water) and R-717 benefit the most from the injection. This can be attributed to the large enthalpy of evaporation of these refrigerants. As explained above, the pressure reduction caused by temperature reduction is counteracted by the added mass. With a large enthalpy of evaporation, only a small amount of liquid needs to be injected to achieve cooling, reducing the detrimental effect of the additional mass. Apart from R-718 and R-717, some efficiency improvement is also achieved for R-32, while for R-134a and R-290 (propane) the injection reduces the efficiency. It is also evident that the injection is more effective for larger temperature lifts and at low evaporation temperatures.

3. TECHNOLOGICAL CONSIDERATIONS FOR SYSTEM COMPONENTS

3.1 Compressor Operating Range

In addition to the reduced compression work, another potential benefit of the liquid injection is the reduction of maximum refrigerant temperatures and the resulting increase of the feasible operating range. To illustrate this, some generic operating limits for reciprocating compressors with the refrigerants R-717, R-134a and R-404A are shown in Figure 5. These operating limits are not specific to a certain compressor model, but are instead a compilation of data from multiple manufacturers (Mayekawa Europe, 2020; Sabroe, 2022; BITZER Kühlmaschinenbau GmbH, 2023; GEA Group AG, 2024; Bock GmbH, 2024). It is evident that the operating envelope for R-717 is fundamentally different from those shown for the synthetic refrigerants. With R-134a and R-404A, the maximum allowable condensing temperature t_c is constant over a wide range of evaporating temperatures t_o, allowing large temperature lifts at low t_o. For R-717, the maximum allowable t_c decreases strongly with decreasing t_o for most of the operating range. This is due to the large discharge superheat that occurs with R-717 and the resulting high discharge temperatures. Elevated discharge temperatures pose significant challenges, primarily due to oil degradation, which accelerates as the temperature rises. It is assumed that the oil aging rate doubles for every 10 K increase in temperature (Bock & Puhl, 2010). Therefore, to avoid premature oil failure, the allowable condensing temperature must be limited.

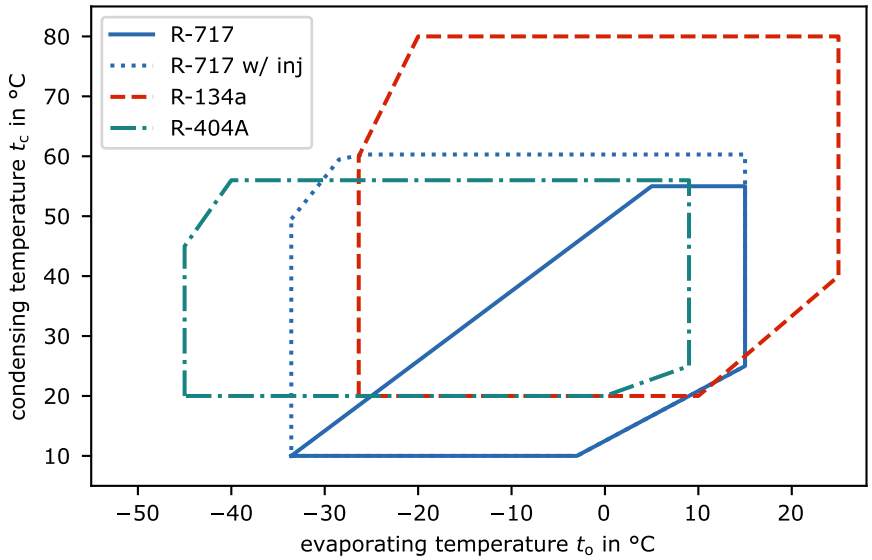

Figure 5: Generic operating limits for reciprocating compressors with R-717, R-134a, and R-404A and theoretical limits for injected R-717 compressor

It is shown in Figure 3 that the liquid injection has the potential to reduce the discharge temperature, based on the amount of injected liquid. With that, the discharge temperature is no longer of concern regarding the operating limits. To show the potential for operating limits resulting thereof, the theoretical limits of an R-717 reciprocating compressor with injection are shown in Figure 5. These limits are based on the assumption that with R-717 the same maximum condensing pressure, pressure ratio, and pressure difference is allowable as with R-134a and R-404A. From this basic evaluation, it is evident that the liquid injection has the potential to significantly increase the operating range for R-717 reciprocating compressors. With the proposed operating limits, single-stage systems with these compressors could be

used for applications such as deep-freezing at high ambient temperatures or space-heating at low ambient temperatures, which are hardly feasible with regular R-717 reciprocating compressors.

3.2 Injection Pump and Injection Pressure Difference

Influence of Pressure Difference on Injection Rate

In section 2.4, some theoretical injection rates were assumed. In reality, the injection rate can only be controlled indirectly as a function of pressure difference and degree of opening. With solenoid injector valves, the degree of opening cannot be controlled. These valves are either completely open or closed and the flow rate after opening is constant for a constant pressure difference, aside from short transient phases during valve opening and closing. Piezoelectric injectors additionally allow controlling the degree of opening (Reif, 2015). For both types of injectors, the volumetric flow rate at full opening depends on the pressure difference. The pressure dependence can be approximated with

$$\dot{V}_{\mathrm{act}} = \sqrt{\frac{\Delta p_{\mathrm{act}}}{\Delta p_{\mathrm{ref}}}} \cdot \dot{V}_{\mathrm{ref}}, \tag{11}$$

where $\dot{V}$ and Δp are the volumetric flow rate and injection pressure difference at a reference point (*ref*) and for the actual operating point (*act*) respectively (Bosch Motorsport, 2019). Because the pressure at the injector inlet is constant and the pressure in the chamber is increasing during the compression stroke, the injection pressure difference is decreasing. The injection rate therefore decreases in the profile of a root function according to equation (11). The pump pressure difference Δp_{pump}, i.e. the difference between pump outlet and condensing pressure, influences the curvature of the injection rate. With a large Δp_{pump}, i.e.

$$\Delta p_{\mathrm{pump}} \gg (p_{\mathrm{c}} - p_{\mathrm{o}}), \tag{12}$$

the injection rate is nearly constant, because the change of injection pressure difference over the compression stroke is negligibly low.

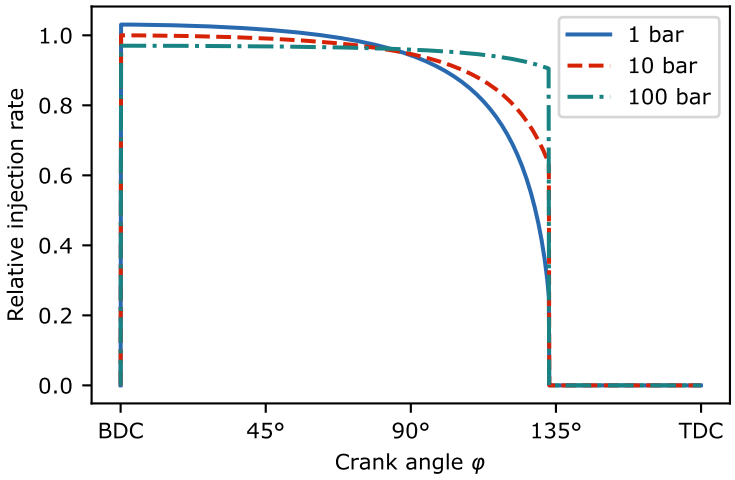

Figure 6: Pressure dependent injection rate for $\Delta p_{\mathrm{pump}} = 1 \ldots 100$ bar (R-717, $t_{\mathrm{o}} = -10\,°\mathrm{C}, t_{\mathrm{c}} = 45\,°\mathrm{C}$)

The coupled compression-injection process is calculated with the pressure-difference based injection rate for $\Delta p_{\mathrm{pump}} =$ 1 bar, 10 bar, 100 bar. The total mass is equal for all pressures and adjusted so that the discharge state is at the dew line. The resulting injection rates are shown in Figure 6, where the pressure dependency as described above is evident. Regarding the compression work, it is found that the indicated work for all pump pressures is equal to the ”dew line” compression within the expected computational tolerance. It can therefore be concluded that the injection pressure does not have a major effect on compression efficiency. It should however be noted that this is merely a theoretical evaluation and the pump work is not included in these calculations.

Influence of Pressure Difference on Atomization

The detailed atomization characteristics of the injected liquid are extremely complex and require specific research in the future. There are however some dimensionless numbers, among others the *Weber* number, which can be used to estimate the influence of injection pressure on droplet breakup. The critical *Weber* number We_{crit} is defined as

$$We_{\mathrm{crit}} = \frac{\varrho \cdot c_{\mathrm{out}}^2 \cdot d_{\mathrm{crit}}}{\sigma}, \tag{13}$$

where ϱ is the density, v_{out} is the velocity at the injection nozzle, d_{crit} is the critical droplet diameter, and σ is the surface tension. The *Weber* number states that every droplet, whose properties are such that the right side of (13) is larger than the left side, will break up into smaller droplets. The critical diameter is therefore the largest diameter with which a droplet can exist indefinitely. For drops larger than d_{crit}, the average time until breakup decreases with an increasing difference $d - d_{\mathrm{crit}}$. The critical *Weber* number depends on the drag coefficient of the droplet, with $We_{\mathrm{crit}} \approx 12$ being a typically chosen value for combustion engines (Lefebvre & McDonell, 2017; Van Basshuysen, 2013).

The outlet velocity can be calculated from the injection pressure difference (Van Basshuysen, 2013):

$$c_{\mathrm{out}} = \sqrt{\frac{2}{\varrho} \cdot \Delta p} \tag{14}$$

With (14), (13) can be written as

$$We_{\mathrm{crit}} = \frac{2 \cdot \Delta p \cdot d_{\mathrm{crit}}}{\sigma}. \tag{15}$$

To evaluate the required pressure difference for the refrigerant injection relative to gasoline injection in combustion engines, it is stipulated that equal values for We_{crit} and d_{crit} are valid for both processes. Under this assumption,

$$\Delta p_{\mathrm{R}} = \Delta p_{\mathrm{F}} \cdot \frac{\sigma_{\mathrm{R}}}{\sigma_{\mathrm{F}}} \tag{16}$$

can be derived, where the indices *R* and *F* denote "refrigerant" and "fuel" respectively. It can be seen that the surface tension has a major influence on the required pressure difference, with Δp_{R} being proportional to σ_{R} in (16). As a reference fuel, n-heptane with $\sigma_{\mathrm{F}} = 20\,\mathrm{mN/m}$ at 20 °C is assumed (Bell *et al.*, 2014). In Table 2, the surface tension for various refrigerants is shown. Additionally, the theoretical injection pressure resulting from (16) for $\Delta p_{\mathrm{F}} = 50\,\mathrm{bar}$, which is a reasonable value for gasoline direct injection engines, is shown. For most evaluated refrigerants, the required pressure is in the same order of magnitude but lower compared to gasoline. Outliers are R-718 with a very large surface tension and R-744 with a very low surface tension. Assuming that refrigerant and gasoline injection are actually comparable, it can be concluded from this data that the required pressures are technically feasible with reasonable effort. For the case of R-744 it seems likely that the difference between condensing and chamber pressure is sufficient to facilitate injection during the beginning of the compression stroke and that a pump may not be necessary.

	t_c = 30 °C		t_c = 60 °C	
Refrigerant	**σ in mN/m**	**Δ*p* in bar**	**σ in mN/m**	**Δ*p* in bar**
R-134a	7,38	18,2	3,74	9,2
R-290	6,43	15,9	3,08	7,6
R-32	6,00	14,8	1,78	4,4
R-404A	3,86	9,5	0,81	2,0
R-717	19,3	47,8	12,7	31,5
R-718	71,3	176,2	66,3	163,9
R-744	58,85E-03	0,1		

Table 2: Surface tension and estimated injection pressure difference at reference pressure $p_{\mathrm{F}} = 50\,\mathrm{bar}$ for various refrigerants (Bell *et al.*, 2014)

4. CONCLUSION AND OUTLOOK

The concept of high-pressure liquid injection for reciprocating compressors is theoretically evaluated using an energetic chamber model. Significant efficiency improvement with certain refrigerants and at large temperature lifts is expected.

The method is particularly suitable for R-717 and R-718, making it interesting for not only refrigeration, but also (high-temperature) heat pump systems. Furthermore, compressor discharge temperatures can be effectively reduced through liquid injection. This opens up considerable potential for extending the application limits of reciprocating compressors, particularly with R-717. First estimations regarding injection pressure difference show the required pressure difference to be feasible.

As the next step, the energetic chamber model is to be validated with experimental data. For optimization of the process, further research regarding the injection and atomization is required. The injection is also promising for transcritical cycles, e.g. with R-744, but detailed evaluation of the effects on cycle efficiency and heat exchanger characteristics is required.

NOMENCLATURE

Symbols			**Subscript**	
p	pressure	(Pa)	chamb	chamber
T	temperature	(K)	gas	gas
t	temperature	(°C)	inj	injection
ϱ	density	(kg/m^3)	sat	saturation
h	specific enthalpy	(J/kg)	mix	mixed
u	specific internal energy	(J/kg)	suc	suction
s	specific entropy	(J/(kg K))	pump	pump
c	velocity	(m/s)	o	evaporation
d	diameter	(m)	c	condensation
m	mass	(kg)	is	isentropic
V	volume	(m^3)	is, it	isentropic-isothermal
$\dot{V}$	volumetric flow rate	(m^3/s)	act	actual
$\dot{Q}$	heat flow rate	(W)	ref	reference
w	specific work	(J/kg)	crit	critical
W	work	(J)	out	outlet
P	power	(W)	R	refrigerant
COP	coefficient of performance	(-)	F	fuel
ε	energy ratio	(-)		
η	efficiency	(-)		
We	Weber number	(-)		

REFERENCES

Abdan, S., Basha, N., Kovacevic, A., Stosic, N., Birari, A., & Asati, N. (2019, August). Development and Design of Energy Efficient Oil-Flooded Screw Compressors. *IOP Conference Series: Materials Science and Engineering*, *604*(1), 012015. doi: 10.1088/1757-899X/604/1/012015

AHRI. (2020). *Standard 540 - Performance Rating of Positive Displacement Refrigerant Compressors.*

Basha, N., Kovacevic, A., & Rane, S. (2021, July). Numerical investigation of oil injection in screw compressors. *Applied Thermal Engineering*, *193*, 116959. doi: 10.1016/j.applthermaleng.2021.116959

Bell, I. H., Groll, E. A., & Braun, J. E. (2011, January). Performance of vapor compression systems with compressor oil flooding and regeneration. *Int. J. Refrigeration*, *34*(1), 225–233. doi: 10.1016/j.ijrefrig.2010.09.004

Bell, I. H., Groll, E. A., Groll, E. A., Braun, J. E., & Horton, W. T. (2013, November). Experimental testing of an oil-flooded hermetic scroll compressor. *Int. J. Refrigeration*, *36*(7), 1866–1873. doi: 10.1016/j.ijrefrig.2013.01.006

Bell, I. H., Wronski, J., Quoilin, S., & Lemort, V. (2014, February). Pure and Pseudo-pure Fluid Thermophysical Property Evaluation and the Open-Source Thermophysical Property Library CoolProp. *Industrial & Engineering Chemistry Research*, *53*(6), 2498–2508. doi: 10.1021/ie4033999

BITZER Kühlmaschinenbau GmbH. (2023, October). *Bitzer Software.*

Bock, W., & Puhl, C. (2010). *Kältemaschinenöle*. Berlin Offenbach: VDE-Verl.

Bock GmbH. (2024). *BOCK VAP.*

Bosch Motorsport. (2019). *Einspritzventile* (Tech. Rep.). Abstatt: Bosch Engineering GmbH.

Cho, H., Chung, J. T., & Kim, Y. (2003, January). Influence of liquid refrigerant injection on the performance of an inverter-driven scroll compressor. *Int. J. Refrigeration*, *26*(1), 87–94. doi: 10.1016/S0140-7007(02)00017-8

DIN e.V. (2013). *DIN EN 12900:2013-10, Kältemittel-Verdichter - Nennbedingungen, Toleranzen und Darstellung von Leistungsdaten des Herstellers; Deutsche Fassung EN_12900:2013* (Tech. Rep.). Beuth Verlag GmbH. doi: 10.31030/1946468

Dutta, A. K., Yanagisawa, T., & Fukuta, M. (2001, September). An investigation of the performance of a scroll compressor under liquid refrigerant injection. *Int. J. Refrigeration*, *24*(6), 577–587. doi: 10.1016/s0140-7007(00)00041-4

GEA Group AG. (2024, April). *GEA RTSelect.*

Holtzapple, M. T. (1989, January). Reducing energy costs in vapor-compression refrigeration and air conditioning using liquid recycle. III: Comparison to other energy-saving cycles. *Ashrae Transactions*, *95*, 199–205.

Kim, T., Lee, C.-Y., Hwang, Y., & Radermacher, R. (2022, July). A review on nearly isothermal compression technology. *Int. J. Refrigeration*. doi: 10.1016/j.ijrefrig.2022.07.008

Kremer, R., Barbosa, J. R., & Deschamps, C. J. (2012). Cooling of a reciprocating compressor through oil atomization in the cylinder. *HVAC&R Research*, *18*(3), 481–499. doi: 10.1080/10789669.2012.646571

Kremer, R., Deschamps, C. J., & Barbosa, J. R. (2008). Theoretical Analysis of the Effect of Oil Atomization in the Cylinder of a Reciprocating Ammonia Compressor. In *International Compressor Engineering Conference at Purdue.* West Lafayette.

Langebach, R., Bradshaw, C., Schmitt, J., & Khan, A. (2024). Isentropic-Isothermal Efficiency for Optimized Compressor Rating. In *27th International Compressor Engineering Conference.* West Lafayette.

Lee, D., Seong, K. J., & Lee, J. (2015, May). Performance investigation of vapor and liquid injection on a refrigeration system operating at high compression ratio. *Int. J. Refrigeration*, *53*, 115–125. doi: 10.1016/j.ijrefrig.2015.01.013

Lefebvre, A. H., & McDonell, V. G. (2017). *Atomization and sprays* (Second edition ed.). Boca Raton London New York: CRC Press, Taylor & Francis Group.

Liang, C., Liu, H., Ziviani, D., Braun, J. E., & Groll, E. A. (2023). Numerical Analysis of a Vapor-Injected Reciprocating Compressor for a Multi-Evaporator Domestic Refrigerator/Freezer Application. In *13th International Conference on Compressors and their Systems.* London.

Mayekawa Europe. (2020). *Betriebsgrenzwerte für Kolbenkompressoren* (Tech. Rep.). Zaventem.

Reif, K. (Ed.). (2015). *Ottomotor-Management im Überblick*. Wiesbaden: Springer Fachmedien Wiesbaden. doi: 10.1007/978-3-658-09524-6

Rouleau, W. J. (1946). *Air compressor* (No. US2404660A).

Sabroe. (2022). *CMO/TCMO 20-30 - HPO 24-26-28 Reciprocating compressor units* (Tech. Rep.). Højbjerg: Johnson Controls Denmark ApS.

Schmitt, J., & Langebach, R. (2024). High-pressure liquid refrigerant injection for reciprocating compressors. *Int. J. Refrigeration*. doi: 10.1016/j.ijrefrig.2024.04.017

Van Basshuysen, R. (Ed.). (2013). *Ottomotor mit Direkteinspritzung: Verfahren, Systeme, Entwicklung, Potenzial*. Wiesbaden: Springer Fachmedien Wiesbaden. doi: 10.1007/978-3-658-01408-7

ACKNOWLEDGMENT

The research project COMPLI on high-pressure refrigerant injection is funded by the Federal Ministry of Education and Research under the grant number 13FH551KX0.